JOURNAL OF APPLIED ELECTROCHEMISTRY **27** (1997) 651–658

Electrochemistry of molten LiCl–KCl–$CrCl_3$ and LiCl–KCl–$CrCl_2$ mixtures

A. COTARTA

Université Polytehnica de Bucarest, Laboratoire d'Electrochimie assistée par Ordinateur, Spl. Independentei 313, 77 206 Bucarest, Romania

J. BOUTEILLON, J.C. POIGNET

Laboratoire d'Electrochimie et de Physicochimie des Matériaux et des Interfaces, UMR 5631 INPG-CNRS associé à l'UJF, ENSEEG, Domaine Universitaire, BP 75, 38402 St Martin d'hères, France

Received 20 January 1996; revised 19 June 1996

Chemical reactions during dissolution of $CrCl_3$ or $CrCl_2$ in molten LiCl–KCL eutectic have been demonstrated to occur, but the nature of the reactions is not yet well understood. Reduction of $CrCl_3$ to chromium metal occurs through two well-characterized electrochemical steps, at approximately + 0.1 and – 0.9 V vs Ag/AgCl. Each step was studied in the 0.025–0.085 molar $CrCl_3$ concentration range, at various temperatures between 375 and 550 °C. The Cr(III)/Cr(II) electron transfer step exhibited reversible behaviour under all the experimental conditions studied. In contrast, the Cr(II)/Cr(0) step could involve Cr(II) adsorbed species and initial chromium electrocrystallization phenomena, mainly depending on the nature of the substrate.

1. Introduction

Analysis of the thermodynamic and kinetic data related to chromium plating reveals that electrodeposition of chromium from aqueous solutions, without hydrogen evolution, is very difficult to achieve [1]. Hydrogen production leads to hardened and bright chromium layers. The development of chromium plating processes from molten salt electrolytes is an alternative [2–4]. Moreover, at high temperatures, intermetallic diffusion is enhanced so that better adherence of the deposits is obtained [2].

Previous investigations of alkali chloride melts as chromium electroplating electrolytes have shown that the chemistry of these electrolytes is simple and yields electrodeposition of high purity metal [2, 3, 7, 9–12]. These mixtures are possible chromium electroplating electrolytes. The stabililty of $CrCl_2$ and $CrCl_3$ solutions in LiCl–KCl binary eutectics have been studied [3, 6, 12]. Data from the literature concerning $CrCl_2$ solubility are varied. A value below 40 ppm at 500 °C was reported by Levy *et al.* [5], who concluded that $CrCl_2$ precipitation followed the first step of the electrochemical reduction of $CrCl_3$. Later however, they measured a solubility as high as 0.026 mol dm^{-3} from the coulometric reduction of a $CrCl_3$ solution [6]. Moreover, a molar solution of $CrCl_2$ was prepared more recently by Lantelme *et al.* [3].

Highly concentrated and stable $CrCl_3$ solutions, up to 0.45 mol dm^{-3}, were obtained by Lantelme *et al.* [3]. These authors assumed that the $CrCl_3$ solubility is dependent on the morphological characteristics of the salt in the solid state, but the $CrCl_3$ solubilization phenomena are not yet fully understood.

As far as the electrochemical processes are concerned, $CrCl_3$ is reduced to the metallic state through a two-step process involving the $CrCl_2$ intermediate species, and some adsorption phenomena of the chlorochromate species on the surface of the electrode have been reported.

Electronic transfer kinetics was studied for both couples. The Cr(III)/Cr(II) exchange was found to be fast, but in the case of the Cr(II)/Cr(0) exchange, a controversy remained. Some authors suggested that the exchange is slow [9, 10]; others thought it to be nernstian [7]. The adsorption of Cr(III) and Cr(II) species on the electrode was postulated [3, 9], but other researchers [5, 7] reported that chromium species adsorption does not play a significant role. In addition, according to White *et al.* [7], the adsorption process could be masked by the electrocrystallization phenomena occurring simultaneously.

Recently, adsorption of the electroactive species was suggested [9], and the formation of an adsorbed layer of Cr(II) at the electrode surface was reported by Lantelme *et al.* [3]. These authors concluded that the reduction process of the adsorbed and dissolved Cr(II) species occurred simultaneously. They used this property to design a pulse deposition procedure which prevented the dendritic growth of the deposit. Levy and Reinhardt [5] reported that $CrCl_2$ has low solubility. They observed that the electrochemical reduction of $CrCl_3$ resulted in irreversible precipitation of $CrCl_2$. A few authors [3, 8, 9, 12] have studied the effect of water, oxygen or fluoride ions upon the electrodeposition process. According to Laitinen *et al.* [8] the hexachlorochromate (III) species reacts reversibly with water:

0021-891X

$$(CrCl_6^{3-}) + H_2O \rightleftharpoons (CrCl_5OH^{3-}) + HCl$$

Then, the electroactive Cr(III) species are converted to an electrochemically inactive species:

$$2(CrCl_5OH^{3-}) \rightarrow (Cl_5CrOCrCl_5^{6-}) + H_2O$$

finally, giving a chromium oxychloride.

According to White *et al.* [7] the sensitivity of chromium(II) electrolytes to oxygen and moisture ensure the formation of Cr_2O_3, and oxide occlusions may occur in the chromium deposits. On the contrary, a beneficial influence of the presence of oxygen in the melt on the structure of the deposit was observed, but not explained, by Benslimane [12]. Fluoride additions have a very small effect on the equilibrium potential of the chromium couples, but have no significant effect on the electrochemical response of the system. The polarization curves, obtained before and after the addition of fluoride ions, remained unchanged.

In this paper the electrochemistry of $CrCl_2$ and $CrCl_3$ is studied in molten LiCl–KCl eutectic, in the 375–550 °C temperature range. The objective is to clarify questions concerning the chromium chloride solubility, the Cr(III) or/and Cr(II) species adsorption on different substrates, the kinetics of the electron exchange for both couples, and also to study chromium electrocrystallization phenomena.

2. Experimental arrangement

The LiCl–KCl eutectic mixtures were introduced into a Pyrex crucible situated inside an air-tight cell described previously [14], then heated and fused under vacuum. Purified argon containing less than 1 ppm O_2 and H_2O was then flushed through the cell during the experiments. The $CrCl_3$ and $CrCl_2$ solutions were prepared by direct addition of weighed amounts of high purity chlorides (Strem Chemical) to the fused LiCl–KCl eutectic, via an argon filled lock chamber.

The working electrode was either a vitreous carbon rod (3 mm diam.), a tungsten wire (1 mm diam.), a platinum or gold wire (0.5 mm diam.). The electrode area was fixed by the length of the electrode in the melt. The counter-electrode was a carbon rod. Potentials were referred to the silver/silver chloride reference electrode (0.75 mol kg^{-1} AgCl solution in the fused LiCl–KCl eutectic). The reference electrolyte was contained in a thin walled Pyrex bulb at the end of a Pyrex tube.

Standard electrochemical techniques (cyclic voltammetry, chronopotentiometry and chronoamperometry) were employed. A universal programmer (model 173, PAR), coupled to an inverse programmer function generator (model 175, PAR) was used as the potential source. A digital oscilloscope (Nicollet 2090) was used for data acquisition.

Table 1. Solubilization of $CrCl_3$ in LiCl–KCl at 406 °C (total amount: 0.044 mol L^{-1})

C_{CrCl_3} / molL^{-1}	2.86×10^{-2}	3.49×10^{-2}	3.49×10^{-2}	3.89×10^{-2}
Time /h	13	24	36	60
% $CrCl_3$ dissolved	64.9	79.3	79.3	86.7

3. Results and discussion

3.1. *Solubility of chromium chlorides*

The solubility of $CrCl_3$ and $CrCl_2$ was studied by measuring the chromium chloride concentration variation after the introduction of the corresponding salts to the melt. Samples of molten electrolytes, taken at fixed times, were dissolved in acidic aqueous solution and analysed by atomic absorption spectrophotometry. Two sets of results are given in Tables 1 and 2.

The dissolution of $CrCl_3$ was found to be slow (Table 1): the concentration of dissolved $CrCl_3$ increased slowly with time, although the resulting $CrCl_3$ concentration was very far from saturation. The flocculation of fine solid particles in the bulk of the melt was observed as soon as solid $CrCl_3$ was added to the melt. We therefore assumed that the solubilization velocity was limited by surface reaction between solid $CrCl_3$ particles and the dissolved chloride ions:

$$CrCl_3\ (solid) + 3(Cl^-) \rightarrow (CrCl_6^{3-})$$

The solubilization of $CrCl_2$ occurred faster than that of $CrCl_3$. From the experiments and the data reported in Table 2, it could be seen that a part of the $CrCl_2$ initially in solution disappeared from the solution yielding fine colloidal particles dispersed in the melt, but nevertheless finally resulting in a solution which remained stable for more than a week. This phenomenon remains unexplained. It may be postulated that the chromium species slowly react with the solvent or with some nonidentified impurities present in the solvent. It was also verified that the $CrCl_2$ solubility was high, since concentrated solutions, up to 0.2 molar, could be prepared.

3.2. *Electrochemical study of $CrCl_3$* solutions

Cyclic voltammetry transients on a platinum electrode (Fig. 1) show that the reduction of $CrCl_3$ to

Table 2. Solubilization of $CrCl_2$ in LiCl–KCl at 439 °C (total amount: 0.027 mol L^{-1})

C_{CrCl_2} / molL^{-1}	2.7×10^{-2}	2.22×10^{-2}	2.21×10^{-2}	2.221×10^{-2}
Time /h	12	24	65	80
% $CrCl_2$ dissolved	100	81.9	81.9	81.9

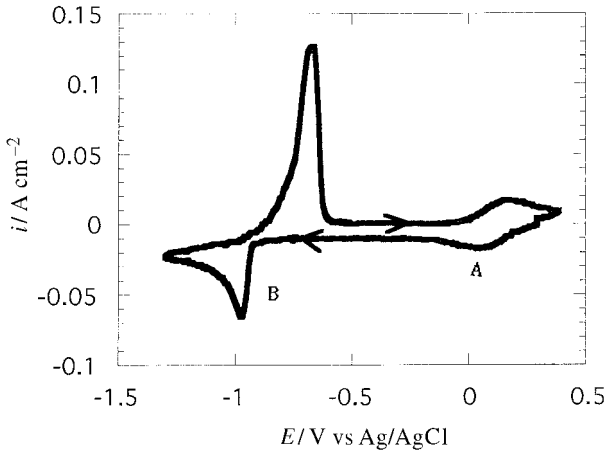

Fig. 1. Cyclic voltammogram for the reduction of $CrCl_3$ in molten LiCl–KCl at 673 K; $v = 0.9$ V s^{-1}; $C_{CrCl_3} = 3.81\times10^{-2}$ mol L^{-1}. Reference: Ag/AgCl (0.75 mol kg^{-1} AgCl in molten LiCl–KCl eutectic). A is Cr(III)/Cr(II) and B is Cr(II)/Cr(0) couples.

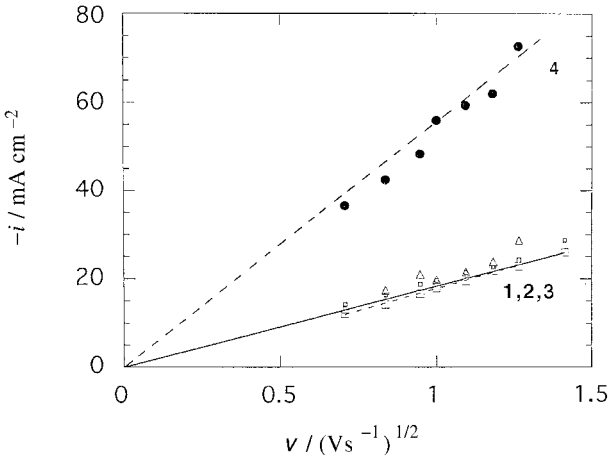

Fig. 3. Variation of the peak current density against the square root of the scan rate. For $C_{CrCl_3} = 2.86\times10^{-2}$ mol L^{-1}. Working electrodes: (1) platinum, (2) gold and (3) vitreous carbon. For $C_{CrCl_3} = 8.57\times10^{-2}$ mol L^{-1}. Working electrode: (4) gold.

chromium metal occurred through two well-separated electrochemical steps, at approximately + 0.1 and – 0.9 V vs Ag/AgCl. These two steps, referred to as A and B, correspond respectively to the Cr(III)/Cr(II) and Cr(II)/Cr(0) couples. Each of these couples was then studied in the 0.025 to 0.085 molar $CrCl_3$ concentration range, at temperatures between 375 and 550 °C.

3.2.1. Cr(III)/Cr(II) couple. The voltammograms presented on Fig. 2 correspond to the reaction:

$$Cr(III) + e^- \rightleftharpoons Cr(II)$$

The curves show that both cathodic and anodic peaks have a symmetrical shape for various values of sweep rate. The data were processed by plotting the cathodic peak currents against the square root of the sweep rate. A typical plot is shown in Fig. 3. The peak currents obtained using gold, vitreous carbon or platinum electrodes were proportional to the square root of the sweep rate and the concentration of $CrCl_3$. These results proved the diffusive character of the exchange process rate-control and also the absence of significant the diffusive character of the exchange process rate-control and also the absence of significant Cr(III) adsorption. Moreover, since the peak potentials did not depend on the scan rate, it can be assumed that the electron exchange process is reversible.

The reduction of the Cr(III) species, as well as the reoxidation of the Cr(II) species, were also studied using chronopotentiometry. The results for the reduction step obeyed Sand's law (Fig. 4) and thus confirmed the diffusion control of the reaction.

The reversibility of the Cr(III)/Cr(II) exchange was confirmed by the convolutional analysis of the voltammograms: the direct and reverse convoluted curves (Fig. 5) corresponding to the voltammograms reported in Fig. 2, were identical whatever the sweep rate. Then, the logarithmic analysis of the convoluted curves was carried out assuming nernstian behaviour:

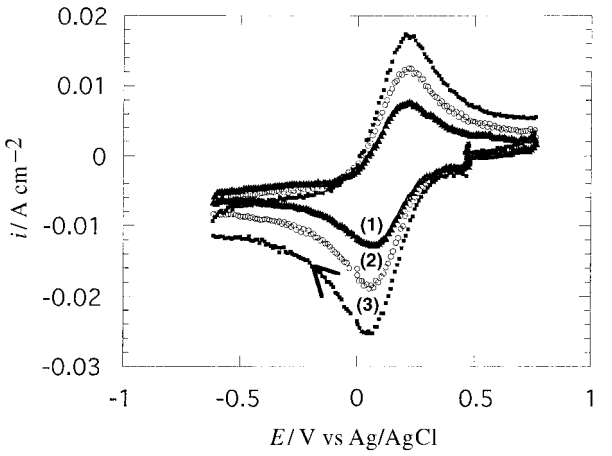

Fig. 2. Cyclic voltammograms for the Cr(III) / Cr(II) electrochemical couple in the fused LiCl–KCl eutectic. $C_{CrCl_3} = 2.86\times10^{-2}$ mol L^{-1}. Working electrode: vitreous carbon. *n*: (1) 0.5, (2) 1 and (3) 1.8 V s^{-1}.

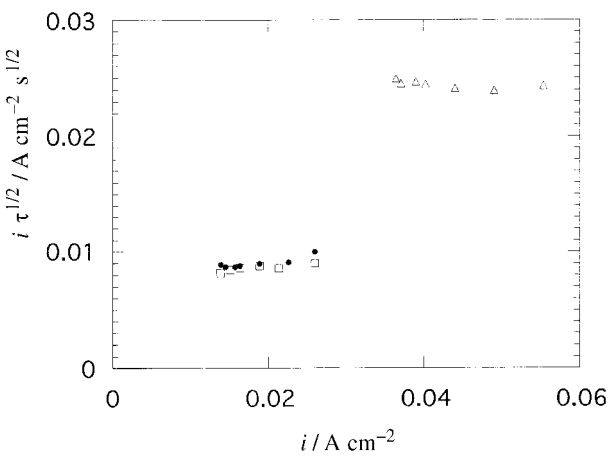

Fig. 4. Sand's law criteria for the Cr(III)/Cr(II) couple: curve $i\tau_1^{1/2} = f(i)$. For $C_{CrCl_3} = 3.81\times10^{-2}$ mol L^{-1} working electrodes: (□) platinum and (•) gold. For $C_{CrCl_3} = 8.57\times10^{-2}$ mol L^{-1} working electrode: (△) gold.

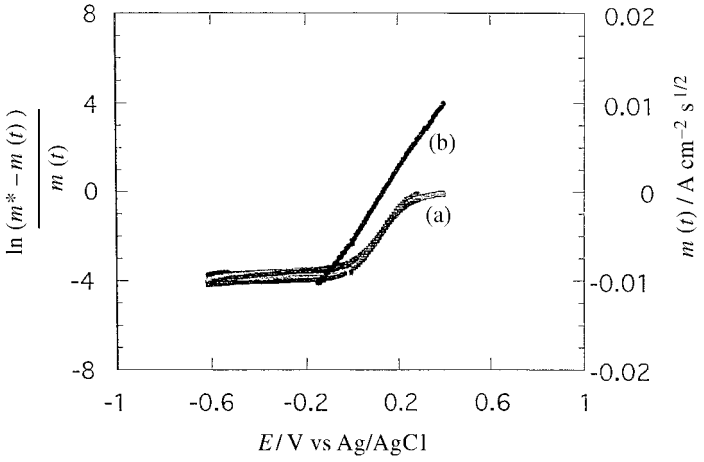

Fig. 5. (a) Semiintegral curves related to the voltammograms of Fig. 2. (b) Logarithmic analysis of a semiintegral curve.

$$E = E_{1/2} + \frac{RT}{nF}\ln\left(\frac{m^* - m}{m}\right)$$

The result is presented in Fig. 5. The slope of the linear part of the curve, equal to 57 mV decade^{-1}, yielded the number of electrons exchanged (i.e., $n = 1$). Similarly the logarithmic analysis of a cathodic chronopotentiogram, according to a nernstian behaviour hypothesis gave a straight line, with a slope of 56 mV decade^{-1} corresponding to a monoelectron exchange. Hence, we concluded that the Cr(III)/Cr(II) exchange is reversible and involves two soluble species.

The diffusion coefficient $D_{Cr(III)}$ was calculated in the 450–540 °C temperature range from the plateau of the convoluted voltammograms using

$$m^* = nFC_{Cr(III)}D_{Cr(III)}^{1/2}$$

The temperature dependence of the diffusion coefficient is represented by an Arrhenius equation:

$$D_{Cr(III)}(\mathrm{cm^2 s^{-1}}) = 1.95 \times 10^{-2}\exp(-6077/T)$$

These values are in agreement with data of Lantelme *et al.* [2]. Assuming that the diffusion coefficients of both soluble species were equal, the apparent standard potential $E^{\circ\prime}$ was assumed to be equal to the half wave potential $E_{1/2}$ (Table 3). As the temperature increased, a positive shift in the Cr(III)/Cr(II) apparent standard potential was observed, which is in agreement with the previous results of Lanteleme *et al.* [3]

3.2.2. Cr(II)/Cr(0) couple. A series of voltammograms related to the reduction of a $CrCl_3$ solution at a vitreous carbon electrode is reported in Fig. 6(a), with the corresponding direct convoluted curves (Fig. 6(b)). The separation of the direct and reverse peak potentials corresponding to the Cr(II)/Cr(0) couple appeared to be larger than expected for a reversible electron exchange. But chromium electrocrystallization phenomena (see Fig. 10) were demonstrated , thus, accounting for the shape of cathodic voltammograms, and also perhaps accounting for the hump at the foot of the oxidation peak. Two plateaux are visible on the convoluted curves, which indicates diffusion control for both steps. From the ratio of these plateaux, $m_2^*/m_1^* = 2$, it may be concluded that the second step corresponds to a two electron exchange. Because of the poor definition of the convoluted curves in the cathodic potential domain, the reversibility of the Cr(II)/Cr(0) electron exchange was not discussed from the analysis of these curves.

At this point, it was merely established that the electrochemical reduction of the $CrCl_3$ solutions occurred following two consecutive steps. The Cr(II)/Cr(0) exchange is not well characterized, and a slow adsorption step of Cr(II) species cannot be ruled out. It was therefore found necessary to carry out a more detailed study of the electrochemistry of $CrCl_2$ solutions in order to improve these results.

Table 3. Apparent standard potential $E^o_{Cr(III)/Cr(II)}$ obtained at different temperatures in LiCl–KCl eutectic melt

Temperature (°C)	375	380	406	455
$E^o_{Cr(III)/Cr(II)}$ ± 0.02 V vs Ag/AgCl	0.16	0.26	0.27	0.3

3.3. *Electrochemical study of $CrCl_2$* solutions

The oxidation and reduction of the $CrCl_2$ solutions were studied by chronopotentiometric and voltammetric techniques. Chronopotentiometry was used to study possible adsorption phenomena, voltammetry and chronoamperometry were mainly employed to discuss nucleation phenomena.

A series of chronopotentiograms related to the oxidation of the Cr(II) ions at a gold (or vitreous carbon) electrode (Fig. 7(a)) were in agreement with Sand's law and provided no evidence of an adsorption phenomenon. The corresponding plots $\tau^{1/2}$ against $I\tau$, at different temperatures (433 °C and 462 °C, respectively), are shown in Fig. 7 (curves (b)). Straight lines through the origin are observed. In addition, the reduction of Cr(II) species at a gold electrode freshly dipped into the electrolyte was proved to be diffusion controlled. Calculation of the

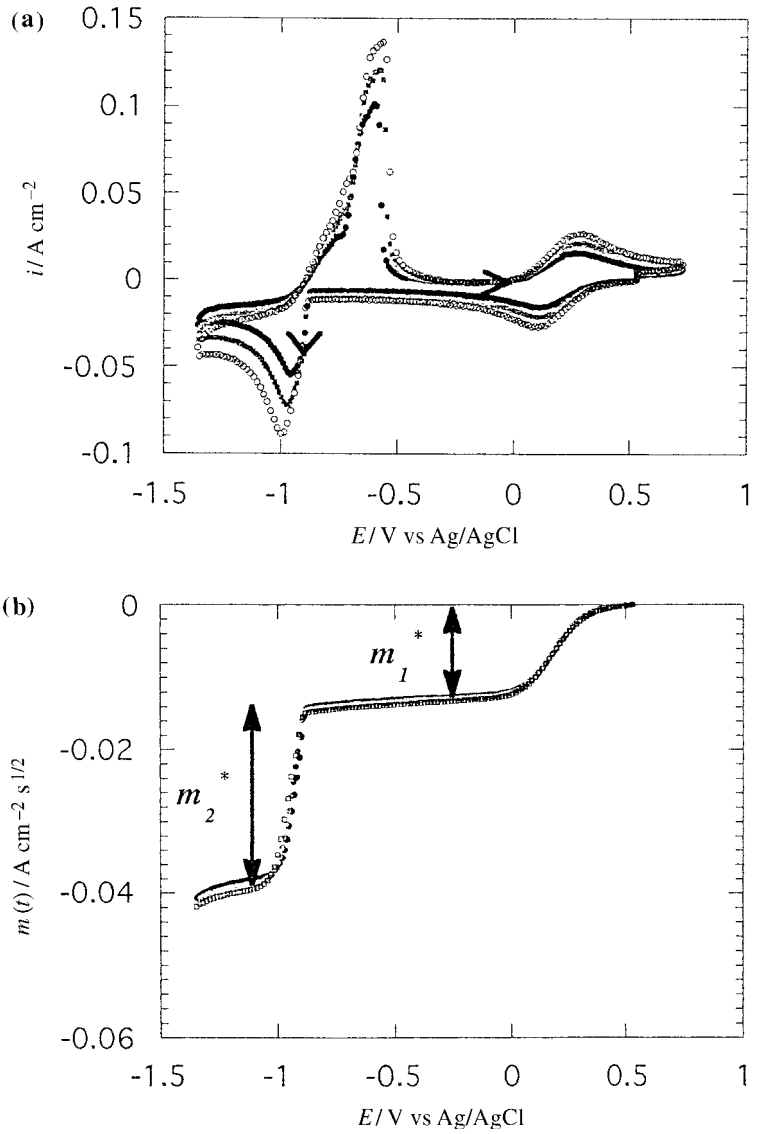

Fig. 6. (a) A series of voltammograms related to the reduction of $CrCl_3$ in the fused LiCl–KCl eutectic at $T = 406$ °C. For $C_{CrCl_3} = 3.49 \times 10^{-2}$ mol L^{-1}, working electrode: vitreous carbon. v: 0.5, 0.9 and 1.4 V s^{-1}. (b) Corresponding direct semiintegral curves.

diffusion coefficient of the Cr(II) ions using Sand's law, yielded values such as $D_{Cr(II)} = (0.62 \pm -0.37) \times 10^{-5} cm^2 s^{-1}$ at 429 °C, which are in agreement with previous data [2, 11].

However, if the gold electrode was immersed a long time in advance, the results were markedly different, and the adsorption of Cr(II) species may be postulated from the chronopotentiometric transients obtained. The analysis of a series of anodic chronopotentiograms, obtained 12 h after immersing the gold electrode, are presented in Fig. 7 (curve (c)). The fact that the extrapolated line, $\tau^{1/2}$ against $I\tau$, does not go through the origin may be attributed to the adsorption of Cr(II) species, the oxidation of which occurs simultaneously with the oxidation of the Cr(II) diffusing species [12, 15].

Adsorption of Cr(II) species on copper and nickel electrodes was also evident: a series of chronopotentiometric transients, related to the reduction of the Cr(II) species, showed that the corresponding $\tau^{1/2}$ against I^{-1} plots (Fig. 8) yielded a positive intercept with the $\tau^{1/2}$ axis.

Finally, in order to investigate whether a Cr(II) adsorption process also occurred on a chromium substrate, a thin chromium deposit (a few micrometre) was plated *in situ* on a tungsten substrate. The electrochemical reduction of a $CrCl_2$ solution was studied on this electrode. A series of chronopotentiograms were obtained and analysed. The value of $I\tau^{1/2}$ was deduced from these experiments, reported in Table 4, and $\tau^{1/2}$ is plotted against I^{-1} in Fig. 8. The product $I\tau^{1/2}$ increased with the current density, which demonstrated the adsorption of the Cr(II) species and the simultaneous reduction of both the adsorbed and dissolved Cr(II) species.

Thus, it may be concluded that the Cr(II) adsorption process depends on the nature of the substrate

Table 4. Sand's law study for the $CrCl_2$ reduction at a chromium-plated tungsten electrode

I/A	0.02	0.03	0.04	0.05	0.06	0.07	0.08	0.09
$I\tau^{\frac{1}{2}}$/As$^{\frac{1}{2}}$	0.0247	0.0251	0.0286	0.0272	0.029	0.0305	0.031	0.032

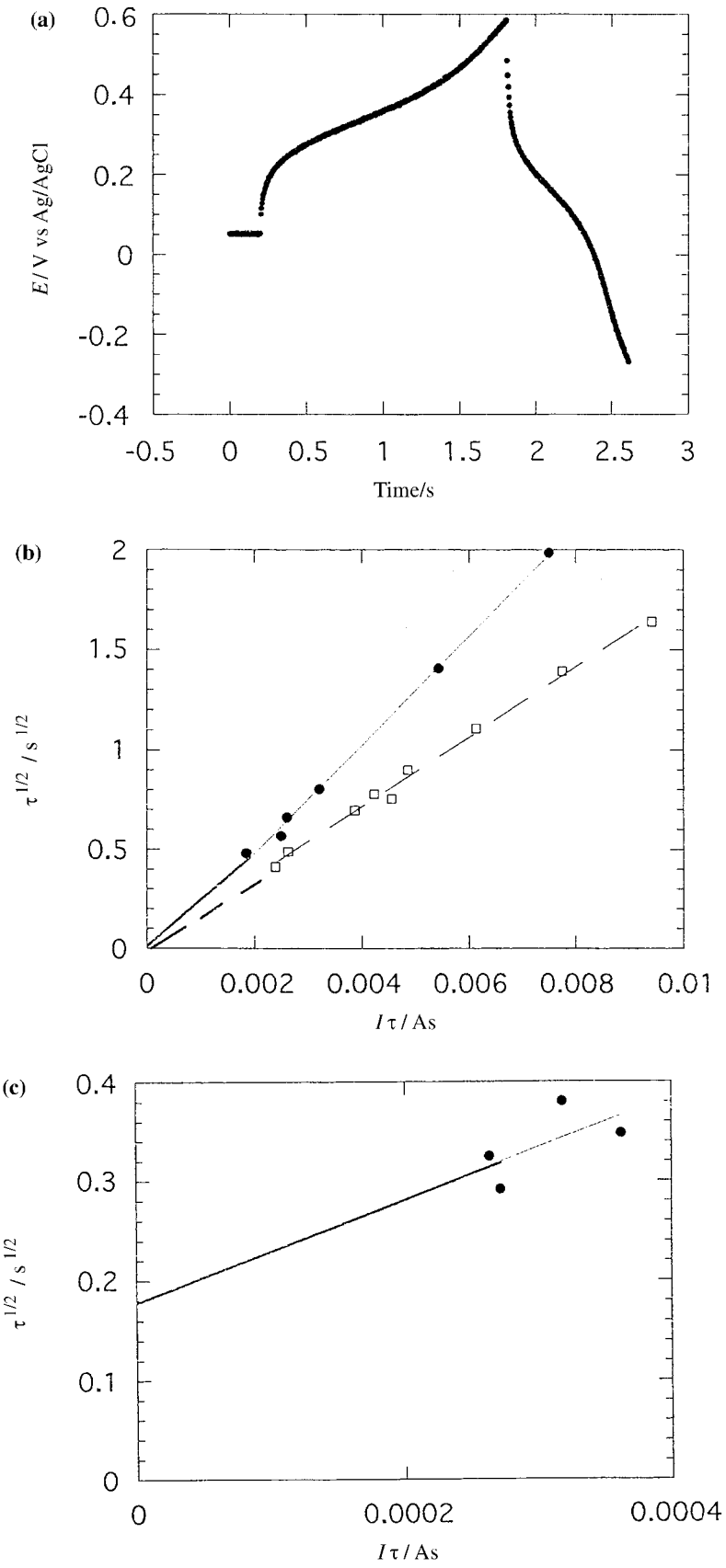

Fig. 7. Chronopotentiometric studies of $CrCl_2$ solution in the fused LiCl–KCl eutectic; $C_{CrCl_2} = 2.97\times10^{-2}$ mol L^{-1}. (a) Current reversal chronopotentiogram; working electrode: gold $i_{pulse} = 0.038$ A cm^{-2}. (b)$\tau^{1/2}$ against $i\tau$ analysis; working electrode: vitreous carbon (1.4 cm^2) at T: (1) 433 and (2) 462 °C. (c)$\tau^{1/2}$ against $i\tau$ analysis; working electrode: gold (0.16 cm^2), dipped into the melt 12h before.

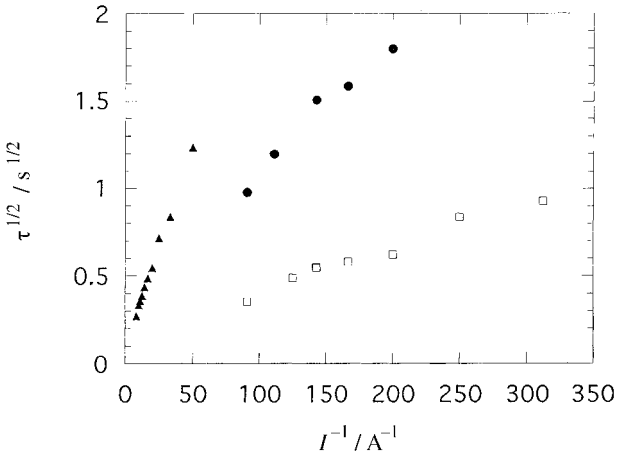

Fig. 8. Chronopotentiometric $\tau^{1/2}\, i^{-1}$ analysis for the reduction of Cr(II). (•)$C_{CrCl_2} = 4.13\times10^{-2}$ mol L^{-1*}, $T = 461$ °C, working electrode: copper (0.32 cm^2); (▲) $C_{CrCl_2} = 9.23\times10^{-2}$ mol L^{-1*}, $T = 431$ °C, working electrode: chromium-electroplated tungsten (0.48 cm^2); (□) $C_{CrCl_2} = 2.89\times10^{-2}$ mol L^{-1}, $T = 431$ °C, working electrode: nickel (0.32 cm^2). * = concentration calculated from the known amount of $CrCl_2$ added.

and also on its interaction with the electrolyte. No adsorption was demonstrated on a vitreous carbon electrode, although a very slow adsorption of Cr(II) species could be detected on a gold electrode and a faster adsorption process occurred at copper or nickel electrodes, as well as at chromium-plated tungsten electrodes.

Cyclic voltammetry was used to investigate the $CrCl_2$ electrochemical reduction, on various cathodic materials, including gold, copper, nickel, vitreous carbon and tungsten. Typical voltammograms are shown in Fig. 9. These curves show that an overpotential was needed for the formation of the first chromium nuclei and that the reverse potential had an influence on the nucleation crossover effect in the reverse $i(E)$ sweep [16]. Chronoamperometric techniques were used to characterize the chromium nucleation process during the electrochemical reduction of $CrCl_2$.

A series of current–time curves, obtained at a vitreous carbon electrode, at different applied over

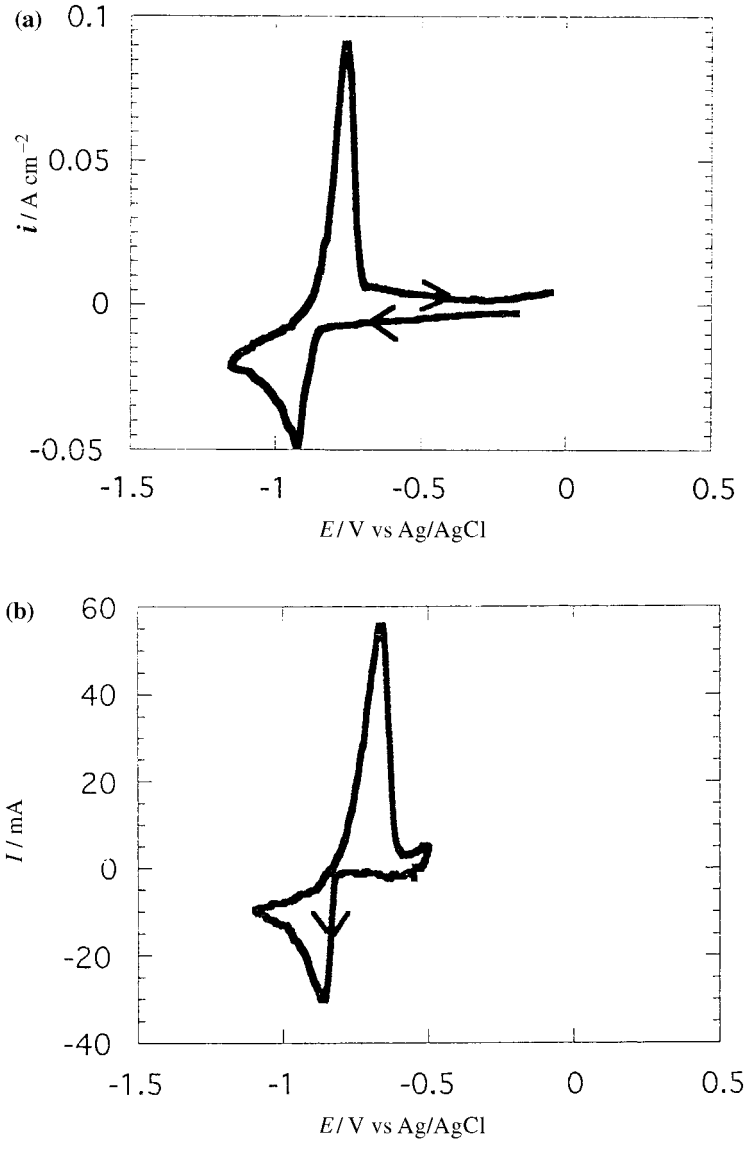

Fig. 9. Cyclic voltammograms for the reduction of $CrCl_2$. (a) $C_{CrCl_2} = 2.71\times10^{-2}$ mol L^{-1}; $T = 489$ °C, working electrode: gold (0.14 cm^2); $v = 0.5$ V s^{-1}. (b) $C_{CrCl_2} = 4.13\times10^{-2}$ mol L^{-1}, $T = 461$ °C, working electrode: copper (0.32 cm^2) $v = 1$ V s^{-1}.

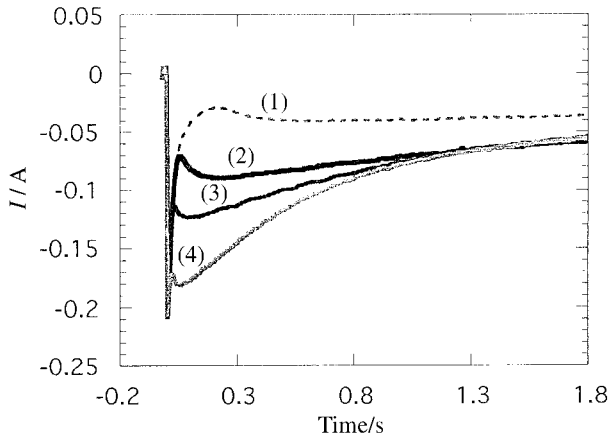

Fig. 10. A series of chronoamperograms for the reduction of $CrCl_2$. $C_{CrCl_2} = 1.76 \times 10^{-1}$ mol L^{-1}*, $T = 414$ °C, working electrode: vitreous carbon (1.4 cm^2). *E*: (1) –0.860, (2) –0.910, (3) –0.970 and (4)1.0 V vs Ag /AgCl. *= concentration calculated from the amount of $CrCl_2$ added.

potentials, are reported in Fig. 10. Their shape is characteristic of the presence of a nucleation process. A variety of theoretical current–potential–time relationships were used to analyse the curves [13], and some preliminary indications were extracted from the behaviour of the current as a function of time in the region prior to the maximum.

The value of $I_{max}^2 t_{max}$ is a convenient criterion to determine whether the nucleation process was instantaneous or progressive. Thus, in the relation $I_{max}^2 t_{max} = Q(zFC)^2 D$, the value of Q is diagnostic [7].

Typical plots of I_{max} against $t_{max}^{-1/2}$, extracted from chronopotentiograms at a vitreous carbon electrode, are shown in Fig. 11. The slope of the linear part was utilized to characterize the nucleation process. The instantaneous nucleation of chromium (Q = 0.14) was demonstrated on a gold electrode, but a progressive nucleation ($Q = 0.4$) process occurred on a vitreous carbon electrode. Consequently, the nucleation process appeared to be controlled by the nature of the substrate and the characteristics of the applied current or potential pulse.

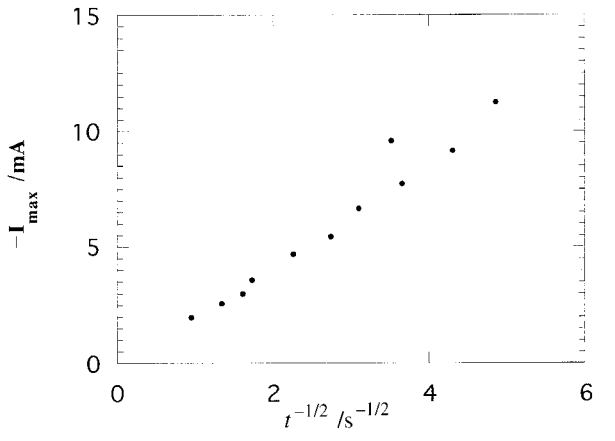

Fig. 11. Chronoamperometric studies of $CrCl_2$ solutions in the fused LiCl–KCl eutectic. I_{max} against $t_{max}^{-1/2}$ analysis. $C_{CrCl_2} = 2.47 \times 10^{-2}$ mol L^{-1}, $T = 428$ °C, working electrode: gold (0.24 cm^2).

4. Conclusion

The present study of the solubility of $CrCl_3$ and $CrCl_2$ in molten LiCl–KCl eutectic has indicated chemical reactions with the solvent. The reduction of the Cr(III) species to chromium was confirmed to occur via a two step process. The reversibility of the first step was confirmed. The results obtained in the study of the Cr(II)/Cr(0) exchange explain some of the discrepancies in previous studies. The behaviour of the Cr(II)/Cr couple appears to be dependent on the 'state' of the solution (achievement of equilibrium could be instantaneous or require a long time), and also on the nature of the material used for the working electrode.

From these results we have designed chromium plating procedures which yield compact and adherent deposits. The next step is the design of a more simple process capable of being scaled up. In this respect, a more precise knowledge and control of the properties of the electrolyte is needed. *In situ* u.v.–visible spectroscopic investigation of the electrolyte, as well as study of the influence of additives on the chemical and electrochemical properties of the electrolyte, will be carried out.

Acknowledgements

The experiments have been carried out at the L.E.P.M.I. (Grenoble, France). Dr Adina Cotarta acknowledges a seven-month fellowship by the French Research Ministry. The experiments were supported by the Copernicus Program of the European Commission project 1177, contract ERBCIPACT 940201.

References

[1] J. Drela, J. Szynkarczuk and J. Kubicki, *J. Appl. Electrochem.* **19** (1989) 933.
[2] T. Vargas and D. Inman, *ibid*, **17** (1987) 270.
[3] F. Lantelme, K. Benslimane and M. Chemla, *Electrochim. Acta* **37** (1992) 1445.
[4] N. C. Cook, *Sci. Amer.* **221(2)** (1969) 38.
[5] S. C. Levy and F.W. Reinhardt, *J. Electrochem. Soc.* **122**(2) (1975) 200.
[6] H. A. Laitinen and C. H. Liu, *J. Am. Chem. Soc.* **80** (1958) 1015.
[7] S. H. White and U.M. Twardoch, *J. Appl. Electrochem.* **17** (1987) 225.
[8] H. A. Laitinen, Y. Yamamura and I. Uchida, *J. Electrochem. Soc.* **125**(9) (1978) 1450.
[9] D. Inman, J. Legey and R. Spencer, *J. Electroanal. Chem.* **61** (1975) 289.
[10] F. Lantelme and El-Hamid Cherrat, *ibid.* **297** (1991) 409.
[11] F. Lantelme, K. Benslimane and M. Chemla, *ibid.* **337** (1992) 325.
[12] K. Benslimane, Thesis, University of Paris VI (1991).
[13] G. Gunawardena, G. Hills, I. Montenegro and B. Scharifker, *J. Electroanal. Chem.* **138** (1982) 225.
[14] J. Bouteillon and A. Marguier, *Surf. Technol.* **22** (1985) 205.
[15] W. Lorentz, *Z. Elektrochem* **59** (1955) 730.
[16] R. Greef, R. Peat, L. Peter, D. Pletcher and J. Robinson, 'Instrumental Methods in Electrochemistry', Southampton Electrochemistry Group, University of Southampton, Ellis Horwood, Chichester (1985).